International Journal of Maritime and Interdisciplinary Research
©2025 IJMIR/Volume 8(1) July-December | ISSN: 2734-3286.

Journal homepage: www.ijmir.edu.ng

DESIGN OF A HYBRID WAVE ENERGY CONVERTER FOR ESCRAVOS USING PHK-ROS MODEL

NWAORGU, G.O[*1], NWAOHA T.C[2] AND AGBAKWURU J.A[3]

[*1]*Nigeria Maritime University, Okerenkoko, Delta State, Nigeria*
Department of Marine Engineering
[23]*Federal University of Petroleum Resources, Delta State, Nigeria*
Department of Marine Engineering

Abstract:

In this research, a hybrid wave energy converter (HWEC) is designed for Escravos deep sea, and its power generation capacity is evaluated. The system is proposed for a combination of WEC and solar power to improve the energy efficiency and reliability. It is supposed to incorporate forty-four WECs and four hundred and forty PV solar panels of 500W each. Wave data and solar irradiance data from the Escravos offshore area were used to evaluate HWEC performance. The WEC is analysed using Port-Hamiltonian Koopman Reduced Order Stochastic (PHK-ROS) model. The PHK-ROS model analysed a maximum of 2641W for one of the WEC floaters, and a total of 116.204kW generated by all forty-four WEC floaters. The period of the wave crest is between 0 and 4.5 seconds. The solar array provides a maximum instantaneous power of 176 kW. Solar analysis shows that there are 5.4 to 6.2 peak sun hours per day on average between November and February. Between May and October, the average hours to receive the sun per day range from 1.3 to 4.12 hours. The total power output result of one WEC floater for different time intervals shows an oscillatory trend variation in the interval from approximately 0 to 2.641kW. The total power produced by the forty-four WEC is 116.2kW. The HWEC patterns indicate that the Solar Plant provides a base load of energy of 10.746 kW. At the same time, the WEC provides the region with dynamic peak power, forming a complementary renewable energy resource for the region of Escravos, with the average combined power of 292.2 Kw

Keywords: Renewable Energy; Wave Energy Converters; Solar Power Plant; and Hybrid Wave Energy Converters

Nomenclature and Abbreviations

L — length (m)
H — Breadth (m)
m— mass (kg)
A— Surface Area (m^2)
$\ddot{x}$ — Acceleration (m^2/s)
F_{exc} — Excitation force (N)
$F_{rad}(t)$ — Radiation force (N)
F_{PTO} (t) — Power take off resistance force
K — Hydrostatic stiffness

* Corresponding Author's Contact – Tel: +234(0)8139389081
E-mail: gpdwise@gmail.com

C — Hydrodynamic damping
H(x) — Total stored energy
R — Semi-definite matrix
Γ_c — Control parameter matrix
w_n — Natural frequency
K_{eff}— Stiffness
M_{eff} — Effective and added mass.
$\beta_1$and α_1 — Coupling gains between the floater and the hydraulic PTO subsystem
γ —Reactive damping adjustment.
z(t) — State vector
B_K and A_K — Koopman-reduced operators
$u(t)$ — Stochastic terms of irregular wave effects and $\xi(t)$
σ_w — Spectral wave variance
W_t — Wiener process of a random sea state
$P_{ROS}(t)$— ROS model power absorption
$P_{wec}(t)$—Power output
Vdc — Voltage of the system
DC — Direct current
Tmin — Average daily sunlight hours
E — Total daily energy in watt-hours
η — Efficiency
E_r— Dialy energy requirement
η_{overal} — Product of component efficiencies
P_p — Peak power
N_s — Current
V_m — Rated voltage of each module
TN_p — Parallel modules
P_p — Module peak power
P_M— Rated peak power capacity
N_s — Number of series modules
TN_M— Total Number of Modules
TN_S— Series modules
TN_p — Parallel modules (TN_P).
P_{WEC} — WEC power output
P_{Sola} — Solar panel output
P_{Total}— Total power output
CF — Capacity factor (CF)
xi — Actual value obtained
yi — Predicted values
n — Number of observations
MEA — Mean absolute error

1.0 Introduction

Driven by issues surrounding climate change, fossil fuel exhaustion, and the need for sustainable development, the need for renewable sources of clean energy is growing in world over markets. A country known to have a lot of wave activity, especially at its shores, has a strong chance at harvesting energy from ocean waves (Strielkoski et al, 2021). Located in the southern region of Nigeria, Escravos is ideally located along the Atlantic Ocean with constant wave action, which is ideal for marine energy exploitation (Ogbeibu & Oribhabor, 2023).

Challenges related to reliability, underdevelopment, efficiency, and adaptation to site-specific conditions affect wave energy conversion (WEC) technology. Specifically designed to fit the characteristics of operation and environment of Escravos, this research highlights the design of the Hybrid Wave Energy Converter (HWEC). The hybrid system uses solar and mechanical conversion processes to achieve maximum energy capture for a variety of wave conditions. The research aims to propose a conceptual design that ensures sustainable energy generation, cost-effectiveness, and durability. The system can keep pace with low-energy wave periods and enhance the output in periods of peak load. This is possible through the exploitation of a hybrid approach. Based on performance metrics such as power output, efficiency, and structural resiliency in marine environments, the design proposed will be evaluated.

Due to concerns about climate change and the exhaustion of fossil fuels, the demand for different sources of clean energy is growing. There is a worldwide effort to combine two or more energy extraction methods, which shows promising results in improving energy extraction and generation of hybrid marine power plants (Cui et al, 2024). Analysis of existing research reveals some of the main trends in site selection and technology development, focusing specifically on wave energy conversion (WEC) technologies.

The ocean wave energy is estimated to be 32,000 TWh/year (Koutrouveli et al, 2021). These resources have led to a large amount of research on WEC technologies to make use of the constant and high-power density ocean waves (Cui et al, 2024). However, the competitiveness of the WEC industry is facing some severe challenges, such as a high levelized cost of energy when compared to other eco-friendly power plants, such as wind and solar (Guo et al, 2021). The ways of overcoming these barriers include, for example, the integration of hybrid systems, including WEC with other renewable energy sources and energy storage solutions (Cao et al, 2017). The hybrid

marine energy system is becoming of significance because of the potential increase in energy production, overall system reliability, and levelized cost (Phillips, 2019). Combining different types of renewable resources can also help to address issues related to the intermittency of single sources and boost the efficiency of energy harvesting (Chen & Wu, 2024).

A key consideration when designing and deploying hybrid power plants is the choice of appropriate site(s) (Del et al, 2024). This process includes identifying an appropriate location for the hybrid systems and renewable energy resources while taking into account a number of factors, such as climate, wave, solar irradiance, and tidal currents. Several studies have been conducted on the integration of WEC and other eco-friendly power plants in particular geographical locations (Khurshid et al, 2024). Hybrid offshore wind and wave energy systems analyzed by Sabzehgar & Moallem (2009) offer an eco-friendly, sustainable method for the generation of power. Global research efforts are concentrated on addressing challenges and possibilities of finding new locations where hybrid marine renewable energy systems can operate efficiently. This particular research will be a union between WEC and a solar power plant, which is planned for the Escravos region of Nigeria.

This study is a unique design and evaluation of a hybrid wave energy converter (HWEC) for Escravos. This power plant is a combination of solar PV and mechanical wave capture, which uses two renewable sources together on one platform to provide more steady and diversified power generation than conventional oscillating water column (OWC) or point absorber systems. The performance of the solar plant is estimated to generate an average of 928.46 kWh per day. Solar PV provides additional long-term reliability by generating power during calm seas, and WECs provide permanent power during nighttime.

This research features a conceptual design and Port-Hamiltonian Koopman Reduced Order Stochastic (PHK-ROS) analysis to simulate energy production. However, the advantages provided according to the conventional WECs prove the potential of hybrid systems to use renewable power in Escravos using this model.

There is still a large gap between region-specific and hybridized designs in the African coasts, such as Escravos, Nigeria, despite the global development in WEC technologies. As Felix et al (2019) notes, for wave climates of temperate/industrialized nations, which have limited ability to adapt to the more complex hydrodynamic and infrastructural issues associated with the sub-Saharan and tropical marine regions, WECs are frequently being developed. Most WECs are

developed to deal with oscillating water columns, overtopping devices, or point absorbers, which, when implemented independently, may not work at an optimal speed in dynamic and less predictable wave climates like that of Escravos.

Current implementations are focused on one conversion principle, either electrical or mechanical, without investigating the additional benefits of hybrid systems as investigated (Ahmed et al, 2022). In particular, under variable sea conditions, hybrid systems can be integrated with several energy capture and conversion elements and can offer a huge performance increase. However, not enough research has been conducted with regard to their potential application in West African waters.

There is an absence of site-specific feasibility studies that include compatibility, environmental data, and maintenance logistics for such an energy system (Majeed et al, 2023). These factors are important if any marine renewable energy solution is to be implemented in practice. The lack of unique models, simulation, and prototype testing efforts in this regard leaves a study gap, which curtails sustainable growth towards the marine energy exploitation in Nigeria.

Current WEC models do not satisfy the specific challenges of hydrodynamic and infrastructural characteristics of sub-Saharan and tropical marine environments (Aderinto & Li, 2018). Many WECs come from the climate conditions of temperate and developed countries and are thus less adaptable to less predictable wave climates such as Escravos. Deployment tends to be biased towards a single conversion principle, overlooking or not investigating hybrid systems, which can enhance the performance in different sea states, by considering different energy capture and conversion mechanisms (Ahamed at al, 2022). Also, site-specific feasibility studies as shown in Fig. 1, which include environmental data such as depth, compatibility, and logistical considerations, are lacking. This research will try to fill these gaps by highlighting the adaptability of WECs in the Escravos sea state.

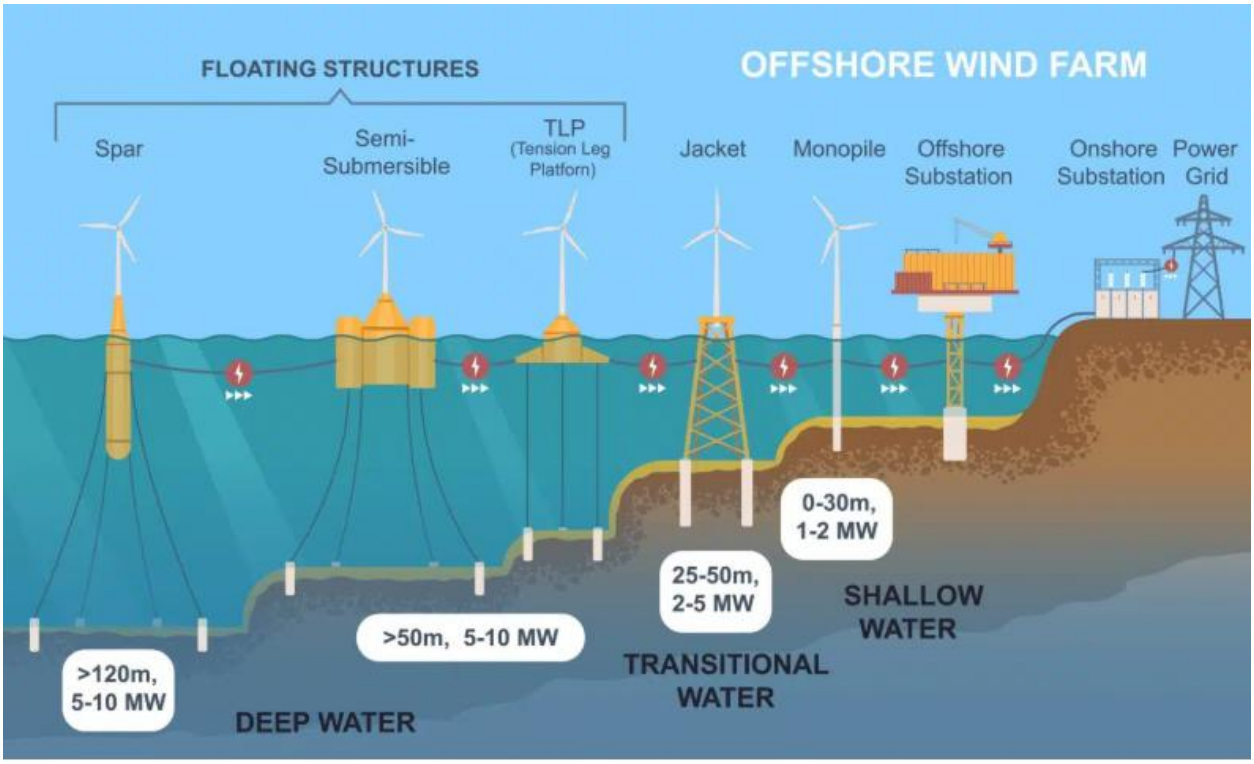


Fig.1 Complexity and Challenges of Floating Renewable Energy due to Water Depth (https://sinay.ai/en/what-is-floating-wind)

The WEC systems along the West African coast were assessed by Ndiaye et al. (2022), with a special focus on the design considerations for different climate conditions. High survivability wave-current hybrid converters' structural optimization was examined by (Ambuhl et al., 2014). Srinivasan and Raghuwanshi (2010) studied the use of a multi-source hybrid coastal marine energy system offshore India by analyzing its performance at various sea states. The design of an HWEC plant for Escravos follows the global trend toward integrating renewable systems for off-grid applications in coastal regions. This study addresses a significant research gap in Sub-Saharan Africa.

This study focuses on a site-specific design and performance simulation using the Escravos region as a case study in order to make a practical and theoretical contribution to hybrid marine power plant setups. Lack of site-specific feasibility study, environmental data, compatibility, and logistical planning are impediments for practical application. Therefore, this research focuses on creating a conceptual HWEC for Escravos. This research will combine the hybrid mechanical-electric energy conversion principles, weather conditions, and local wave data to provide a

potential solution. The resulting design is anticipated to contribute to WEC design by using the PHK-ROS model.

2.0 Methodology

Fig. 2 shows the HWEC 3D model, which integrates solar and wave energy harvesting systems in the same platform. The structure is fitted with four hundred and forty photovoltaic panels (each 500W, and each 29kg). The HWEC holds forty-four floaters of 29kg each. These panels are positioned in such a way as to ensure maximum HWEC exposure to the sun and, at the same time, respect the floating structure equilibrium. The HWEC structure incorporates forty-four WEC floaters distributed along the side of the platform. These floaters are designed to oscillate in response to Escravos wave action, converting mechanical motion to electricity.

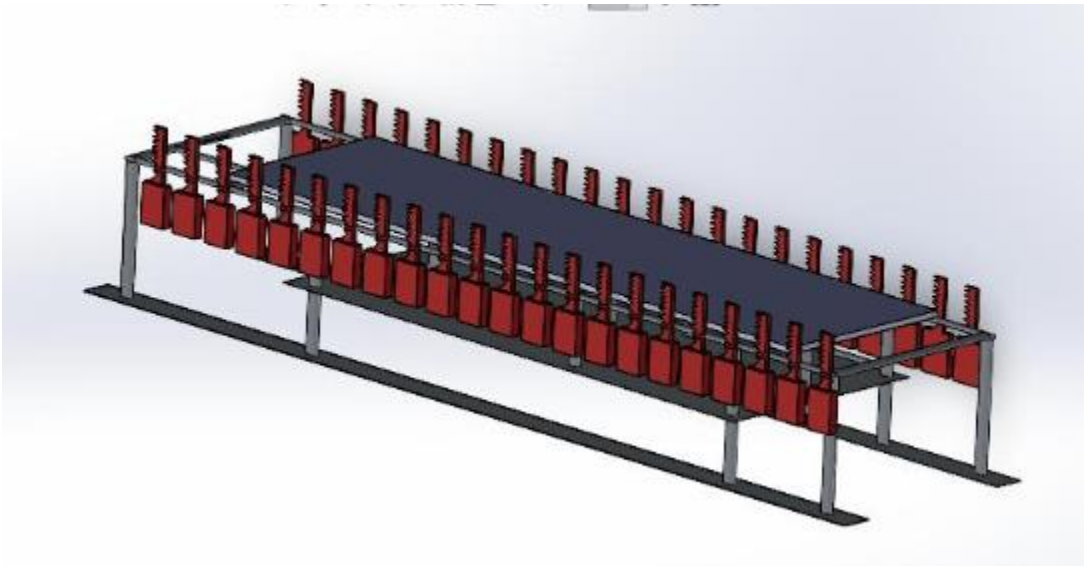


Fig.2 3D Model of the Hybrid Wave Energy Converter

Fig. 2 shows the top view, side elevation, and the entire assembly drawing of the HWEC design. The length overall of the HWEC platform is 71.99m, and its breadth is 14.4m. The top view shows the PV arrangement, while the side view emphasizes the WEC floaters arrangement and its mounting positions. The specifications and configurations of the HWEC major component are shown in Table 1.

Table 1: HWEC Structure Parameter

Floating Structure Type	Hybrid Wave Energy Converter (HWEC)
HWEC length (m)	71.99
Breadth (m)	14.4
HWEC mass (kg)	53332.98
HWEC displacement m^3	386.54
Wetted Surface Area m^2	7450.90

The primary components that will be assembled are shown in Fig. 3, and they are: the HWEC dimensions, floater, and the solar photovoltaic panel size. Given below are the detailed design and the appropriate size computation. For all design analysis and simulation related to the size and shape of the structure, solar PV panels, and floaters, ANSYS Workbench has been used (Silverio et al, 2018).

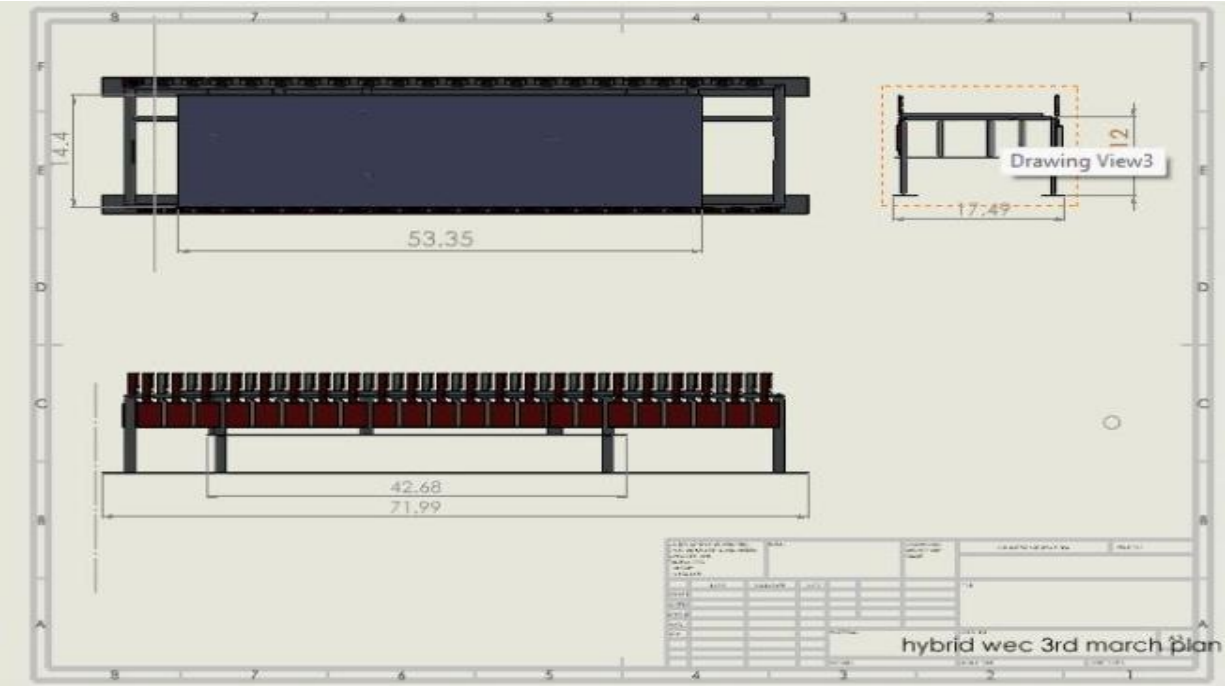


Fig 3: Hybrid Wave Energy Converter Design Dimensions

2.1 WEC Power Generation

This research will adopt the PHK-ROS method, as shown for a point mass in Fig. 4. This is a novel combination of ideas tailored to model the power generation of the WEC. The PHK-ROS is a

hybrid model that will be used to describe the WEC. This model is selected because it uses three complementary model, like energy-based Port-Hamiltonian dynamics, Koopman operator linearization and Reduced-Order Stochastic (ROS) modelling. This model is proposed to provide increased accuracy, computational efficiency and robustness against environmental uncertainty. Traditional WEC models like linear potential theory, Euler theory and Cummins equation are limited when dealing with nonlinear hydrodynamic stochastic wave forcing and real-time turning resonance, whereas the PHK-ROS model will analyse such waves by using:

- Port-Hamiltonian (PH) structure to carry out a full energy-preserving representation
- Koopman theory will analyse the linearization of the nonlinear response of an infinite observable space dimension
- Reduced-Order Stochastic will analyse sea randomness that will preserve the wave properties of Escravos region

The WEC is exposed to irregular wave excitation in the Escravos region, showing a significant wave height (H) of 1.0m, a wave period (T) of 14.29s, a time step (Δt=0.01s) over a duration of 400s, and a depth of 50m was used to ensure stability of both the port-Hamiltonian and Koopman subsystems. The reduced-order stochastic component uses spectral filtering to obtain excitation signals while preserving the peak spectral frequency, wave variance, and the correlation structure of the Escravos region sea state. This process will ensure that the model reflects Escravos wave variability adequately. The WEC has a total of forty-four (44) floaters, of which one weighs 1.5Kg; its added mass is $a_{\infty} = 0.615kg$; its effective mass Meff=2.115kg; and the total damping C_{total}=0.232Ns/m. The Port-Hamiltonian equation for instantaneous power will be expressed as

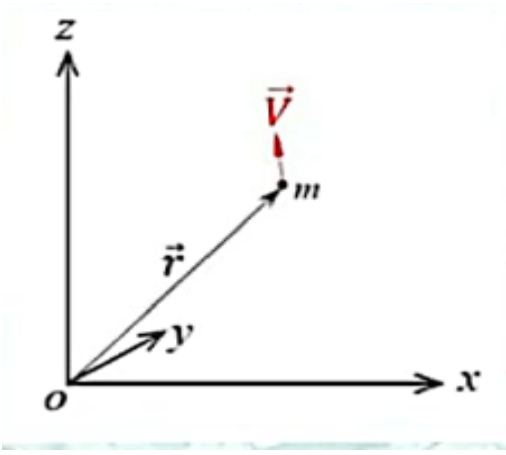


Fig 4: WEC Point Mass

$$P(t) = y^T(t)u(t) \quad (1)$$

Where u(t) is the wave excitation port input, y(t) is the port velocity output, and $\dot{x}(t)$ is the heave velocity.

$$u(t) = F_{exc}(t) \quad (2)$$

$$y(t) = \dot{x}(t) \quad (3)$$

The input power delivered (P_{pH}) by the wave using the Port-Hamiltonian model will become

$$P_{PH}(t) = F_{exc}(t)\dot{x}(t) \quad (4)$$

F_{exc} is the excitation force, while the F_{PTO} (t) is the power take-off resistance for the Port-Hamiltonian model will be expressed as (Korda & Mezic, 2018).

$$F_{PTO}(t) = -\frac{\partial H}{\partial x} R_{mod}\dot{x}(t) \quad (5)$$

$$R_{mod} = R + \Gamma c^T \Gamma_c \quad (6)$$

Where

$\frac{\partial H}{\partial x}$ is the energy gradient, R=0.116Ns/m is the base PTO damping coefficient, and R_{mod} is the modified damping.

The Koopman reduced-order model will be used to linearize the hydrodynamic system into an infinite-dimensional observable space. The Koopman model will be expressed as (O'Dwyer & Ringwood, 2020).

$$\dot{z}(t)A_K z(t) + B_K u(t) + u(t) \quad (7)$$

Where

z(t) is the Koopman state vector, B_K and A_K are the Koopman-reduced linear operators and $u(t)$ is the stochastic terms of irregular wave effects and $u(t)$ is expressed as

$$u(t) = \sigma_w W_t \quad (8)$$

The physical velocity using the Koopman model is

$$\dot{x}(t) = C_k z(t)$$

Where

σ_w is the spectral wave variance, W_t is the Wiener process of a random sea state, C_k is the matrix reconstruction of the Koopman state to physical velocity (Bhattacharyya, 2021).

The ROS-based reactive control model will introduce Γ_c which is a control parameter matrix that will help to adjust the resonance of the system in real time. The resonance condition is given b

$$w_n^2 = \frac{K_{eff}}{M_{eff}} \tag{9}$$

Where

$w_n = \sqrt{\frac{K}{M_{eff}}} = 0.448$ is the natural frequency, $K_{eff} = K + \gamma_{heave} = 0.71N/m$ is the stiffness and M_{eff}=2.115kg is the effective and added mass. The control matrix I expressed as

$$\Gamma_c = \begin{bmatrix} \alpha_1 & \beta_1 & 0 \\ -\beta_1 & \alpha_2 & 0 \\ 0 & 0 & \gamma \end{bmatrix}$$

Where

$\beta_1 = 0.08$ and $\alpha_1 = 0.21$ are the coupling gains between the floater and the hydraulic PTO subsystem, and $\gamma = 0.14$ This is the reactive damping adjustment. The Port-Hamiltonian matrix modulates at J and dissipates at R, as shown

$$K_{eff} = k + \Gamma_c \tag{10}$$

And

$$C_{eff} = R + \Gamma c^T \Gamma_c \tag{11}$$

Where

K=0.21N/m and $C_p = 0.116Ns/m$ are the hydrostatic restoring stiffness and damping, $C_{eff} = C_p + \gamma_{heave}^2 = 0.366Ns/m$ and $K_{eff} = C_p + \gamma_{heave} = 0.71N/m$ are the ROS action effective damping, and ROS resonance tuning stiffness.

The ROS model of power absorption will be expressed as (Falnes, 2002).

$$P_{ROS}(t) = C_{eff}\dot{x}^2(t) + K_{eff}x(t)\dot{x}(t) \quad (12)$$

The power output $P_w(t)$ of the WEC using PAIK-ROSS will be expressed as

$$P_{wec}(t) = F_{exc}(t)\, C_k z(t) + C_{eff}(\, C_k z(t))^2 + K_{eff}x(t)\, C_k z(t) \quad (13)$$

This segment gives a well-informed framework for analyzing WEC dynamics using the PHK-ROS model. The proposed approach provides an optimized WEC design and operation, and an efficient wave energy extraction. The origin of the wave is from the Escravos region with a significant wave height of 1.0m and a period crossing of 14.29s (Abam et al, 2017).

2.2 Solar Power Generation

The dimensions of the PV array are determined both from a financial and a technical point of view. It was argued by Podder et al (2015) that radiation received by a panel is proportional to the panel output. Parameters to be calculated are the size of the panel used to generate the system, the voltage (Vdc) of the system, direct current (DC), average daily sunlight hours (Tmin), and the total daily energy (E) in watt-hours. As soon as these parameters are known, sizing can take place, using a PV panel of 440W. The technical requirements proposed for the PV panel are an advanced cell efficiency of about 30%, advanced minimal sunlight technology efficiency, a 25-year warranty, and a high charging current.

2.2.1 Peak Power

The estimated energy output of the PV panel is given by equation 14, where P is the required power and Tmin is the average number of hours of sunlight per day (Nwaorgu & Ogbonnaya, 2023).

$$\mathrm{E_{rough}} = P * \mathrm{T_{min}} \quad (14)$$

To prevent under-sizing, we start by applying equation 15 to get the daily energy required from the solar array. This involves dividing the overall average energy (E) demand per day by the efficiency (η) of the system components (Khatib & Muhsen, 2020).

$$\frac{E}{\eta} = E_r \quad (15)$$

Where E_r is the dialy energy requirement, E is the dialy average energy consumption, and η_{overal} is the product of component efficiencies as shown in equation 16.

$$E_r = \frac{E}{\eta_{overall}} \quad (16)$$

To determine the Peak power (P_p), equation 14 is divided by the average sun hour per day $T_{min,}$ for the geographical location as shown in equation 17.

$$P_{peak} = \frac{\text{dialy energy requirement}}{\text{average sun hours per day}}$$

$$P_{peak} = \frac{E_r}{T_{min}} \quad Kwp \tag{17}$$

To calculate the peak sun hours (Dumkhana & Idoniboyeobu, 2018),

$$T_{min} = \frac{\text{Average Monthly Solar Power}}{12} \tag{18}$$

The solar panel power generated for t = 1s will be analysed as

$$total\ energy\ per\ sec = \frac{T_{min} * 1000 * number\ of\ panel * Panle\ Power\ Output}{24 * 3600} \tag{19}$$

2.2.2 Number of Series (N_s) and Parallel (N_P) Modules

It is necessary to determine the number of parallel and series modules because the modules should be linked in both parallel and series to provide the required current (N_s) and voltage, which is equal to the DC voltage of the system (V_{DC}) divided by the rated voltage of each module V_M to obtain he string length of the module. Therefore, TN_s is the string of modules in series (Franklin, 2017).

$$TNs = \frac{V_{DC}}{V_M} \tag{20}$$

Calculating the parallel modules (TN_P) which is equal to the module peak power (P_P) divided by one module's rated peak power capacity (P_M), and then multiply the result by the quantity of series modules, then multiply by the number of series modules (Ns) as shown in equation 21.

$$TN_p = \frac{P_P}{P_M * TN_S} \tag{21}$$

Total Number of Modules (TN_M) equals the series modules (TN_S) multiplied by the number of parallel modules (TN_P) as shown in equation 22 (Choi et al, 2011). The calculation overhead is for a 500W load, and with a life PV span of twenty-five years (25 years).

$$TN_m = TN_p * TN_S \tag{22}$$

2.3 HWEC Power Output

It is necessary to consider the individual power generation equations to combine the power output of a wave energy converter (WEC). Using Equation 13, the WEC power output P_{WEC} is

determined, and on the other hand, using Equation 19, the solar panel output P_{Solar} is calculated. The total power output P_{Total} is now calculated as the addition of both contributions. This equation assumes synchronous operation and minimal losses in integrating the systems, ensuring a steady hybrid energy supply.

$$P_{total} = P_{WEC} + P_{Solar} \quad (23)$$

2.4 Result Validation

Mean absolute error and capacity factor will be used for this research validation to assess the HWEC result performance. Various related literature will be used for comparison with the results obtained using MATLAB. The mean absolute error will be used to summarise the average deviation of the different results. Also, it calculates the average error between the predicted and the actual value (Jierula et al, 2021). The capacity factor (CF) is the ratio between the average annual power produced and the rated power capacity of the power plant.

$$MAE = \frac{1}{n}\sum_{i=1}^{n}|y_i - x_i| \quad (25)$$

Where:

xi is the actual value obtained

yi is the predicted values

n is the number of observations

$$CF = \frac{Annual\ Energy\ Production}{Rated\ Power \times 8760h/year} \quad (26)$$

3.0 Results and Discussion

3.1 Results

Fig. 5 shows that the PHK-ROS power output from the WEC varies over time. From 0 to 1 second, the power generated remains relatively low due to a lack of wave motion, resulting in a lower energy transfer efficiency from waves to the WEC. The results demonstrate enhanced resonance between the WEC and wave motion. From 1 to 3 seconds, the power increases significantly to 2,641 W.

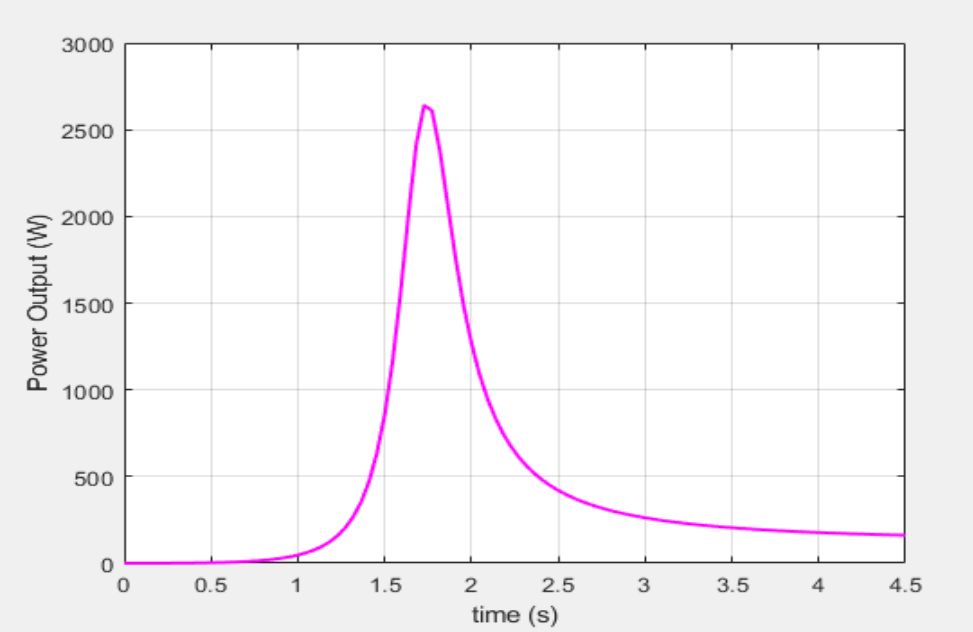


Fig.5 WEC Power Output

Table 2 shows the average daily sunlight hours for more than six years (2018 - 2023) in each month, highlighting clear variations in solar energy potential throughout the year. The energy output of four hundred and forty (500W) solar panels directly depends on sunlight hours, which are affected by seasonal and annual trends. Using the equations between 14 and 22, simulations were conducted with MATLAB software to analyze the solar output, assess the variability of solar irradiance, evaluate the system's performance, and determine the total energy production.

Table 2 indicates the maximum sunshine per hour at Escravos Deep Offshore (NIMET)

Months	2018 (hrs)	2019 (hrs)	2020 (hrs)	2021 (hrs)	2022 (hrs)	2023 (hrs)
January	4.0	6.2	4.8	4.4	4.41	4.3
February	6.0	3.7	4.9	5.53	5.52	4.4
March	4.5	5	5.7	4.8	4.87	4.31
April	5.9	3.9	4.4	4.4	4.5	3.80
May	5.1	4.5	5.1	4.02	4.02	4.49
June	4.0	3.9	1.8	3.7	3.74	2.31
July	3.1	2.8	1.4	3.33	3.34	3.45
August	3.3	2.2	1.3	2.38	2.3	3.63
September	2.6	3.1	2.0	3.3	3.85	3.56
October	4.0	4.0	4.1	3.85	3.33	4.12
November	6.2	6.2	5.8	5.4	5.44	5.3
December	5.6	6.1	5.4	5.75	5.76	5.66

Fig. 6 shows the average hours of sunlight of this region. This season provides a steady and significant supply of energy, and this means that solar panels can perform better and also provide adequate energy to meet most basic needs.

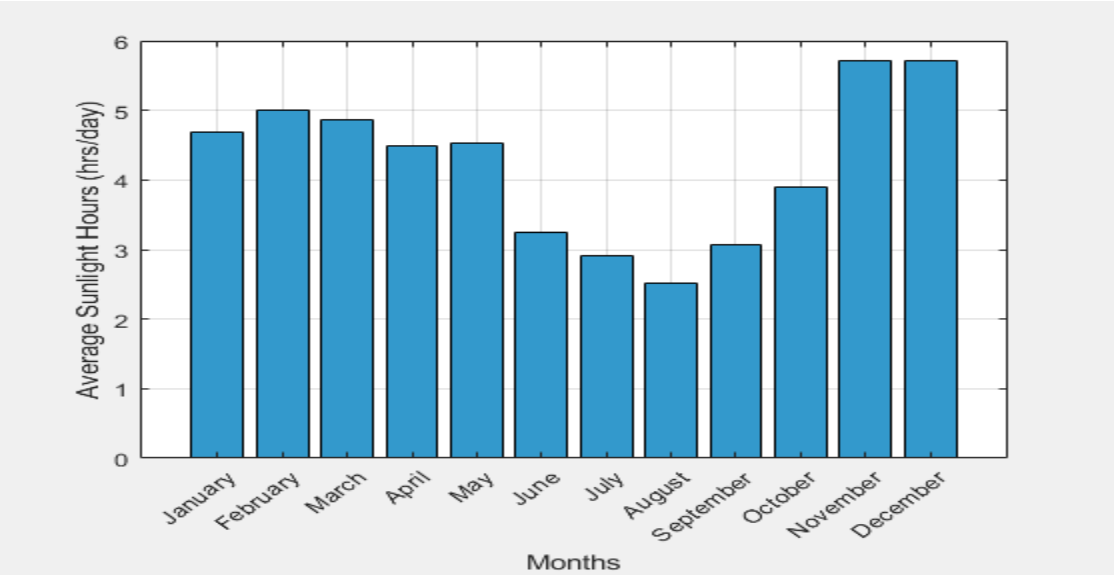


Fig 6 Average Sunlight Hours

Fig. 7 illustrates a stable power output of around 10.746 kW during the analyzed time, which shows constant system performance. With four hundred and forty (500 W) solar panels, the system is capable of producing 176 kW of power. The power output per day for an average of 4.22 sun hours per day is about 928.46 kWh/day. The 10.746 kW is the average power output for 24 hours.

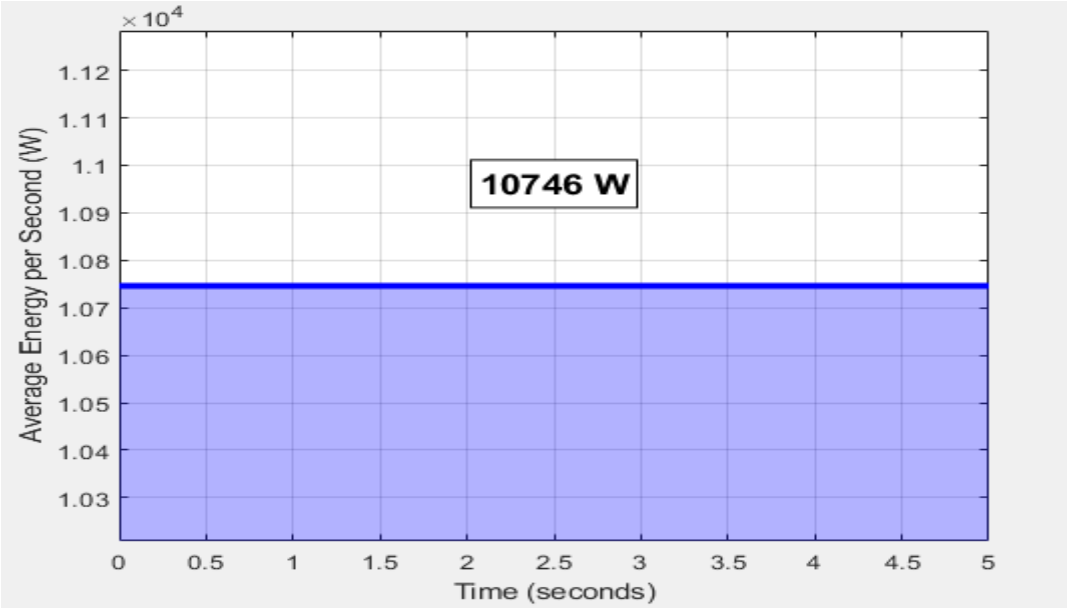


Fig. 7 Average Solar Power Output Over 24hrs

Fig. 8 shows an example of the monthly solar production of the HWEC system compared with a fixed baseline system that is producing 28600kWh per month. The HWEC system is more efficient than its baseline system between October and May, with a maximum output of 39,000kWh in December. From June through September, solar power production decreases considerably, being lowest in August at 17 000kWh, due to a lack of irradiance.

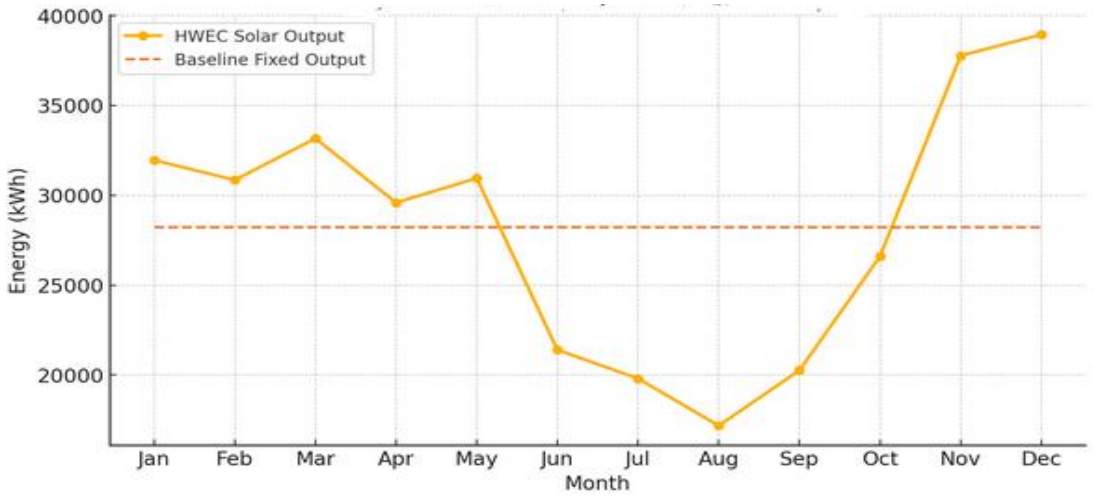


Fig 8 Monthly Solar Energy Generation Comparison

Fig. 9 presents the variation of solar energy output among the months having the least and maximum peak sun hours of August and December, respectively, as presented in Table 2. August output varies from 286.0kWh to 792.6kWh from 1.3 peak sun hours/day to 3.63 peak sun hours/day with a capacity factor of 10.493% which is its lowest value. December always displays higher energy production than other months, with energy production varying from 1,188.0kWh to 1,342.2kWh, peak sun hours are between 5.4 to 6.1 hours/day, and the highest capacity factor is 23.847%. This analysis emphasizes the importance of taking into account solar resource variability in system design.

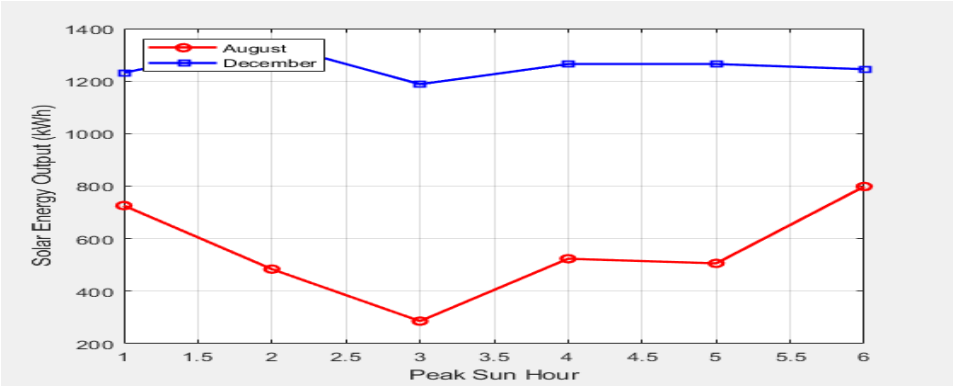


Fig 9 Solar Power Output in August and December

Fig. 10 shows the total power output in time per second with a special focus on an oscillatory output between roughly 10.746kW and 126.95kW over 4.5 seconds. This trend is the sum of a solar power plant and a wave energy converter (WEC), two contributing elements for the energy production. The average solar power required to generate 10.746kWh of energy from the sun over a 24-hour time span is 10.746kW, which is the constant power output that the solar plant provides and can be seen in the output graph below. The oscillatory nature is due to the contribution of the WEC. As the WEC relies on the periodic motion of waves, which is used to generate power, it has a fluctuating output.

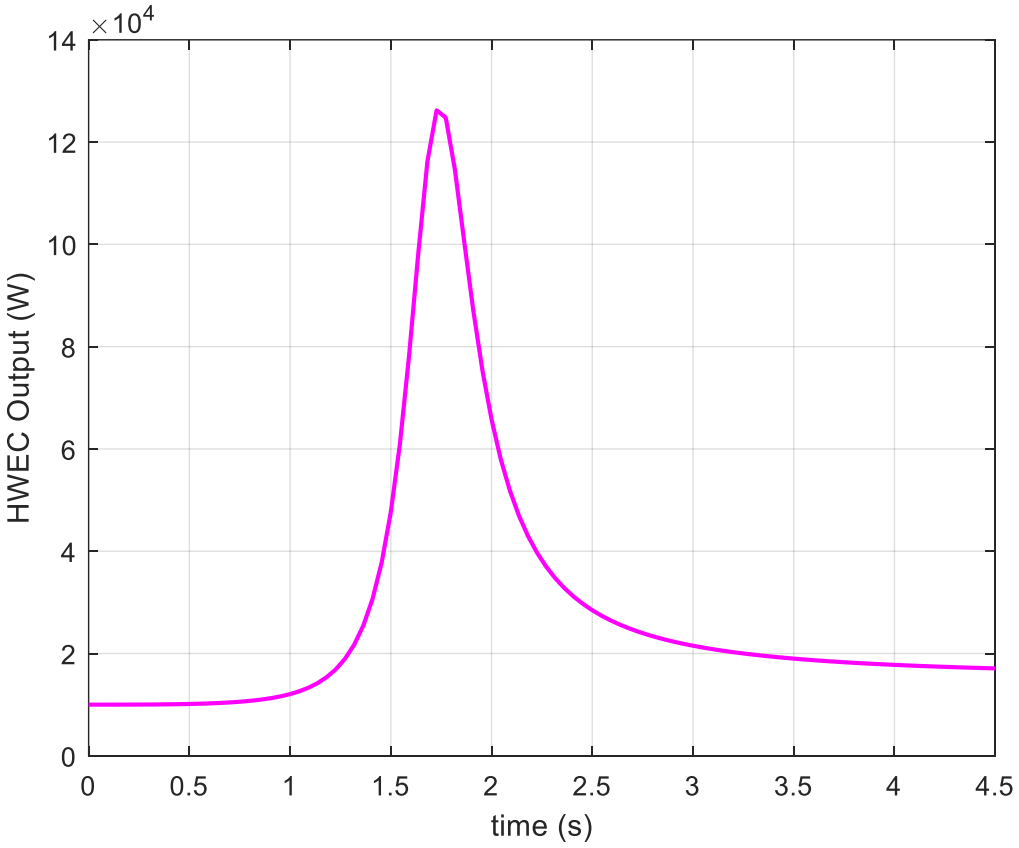


Fig 10 Total Power Output of the HWEC Produced

Fig. 11 illustrates the total power output of the HWEC system wherein the combined power output is 292.2kW and the annual energy production is 1035 MWh/year. The solar panels had a contribution of 26.2%, and the WEC contributed 73.8% (the WEC is more useful than the solar panels because it is the constant availability of waves and the sun is not always there, such as at night).

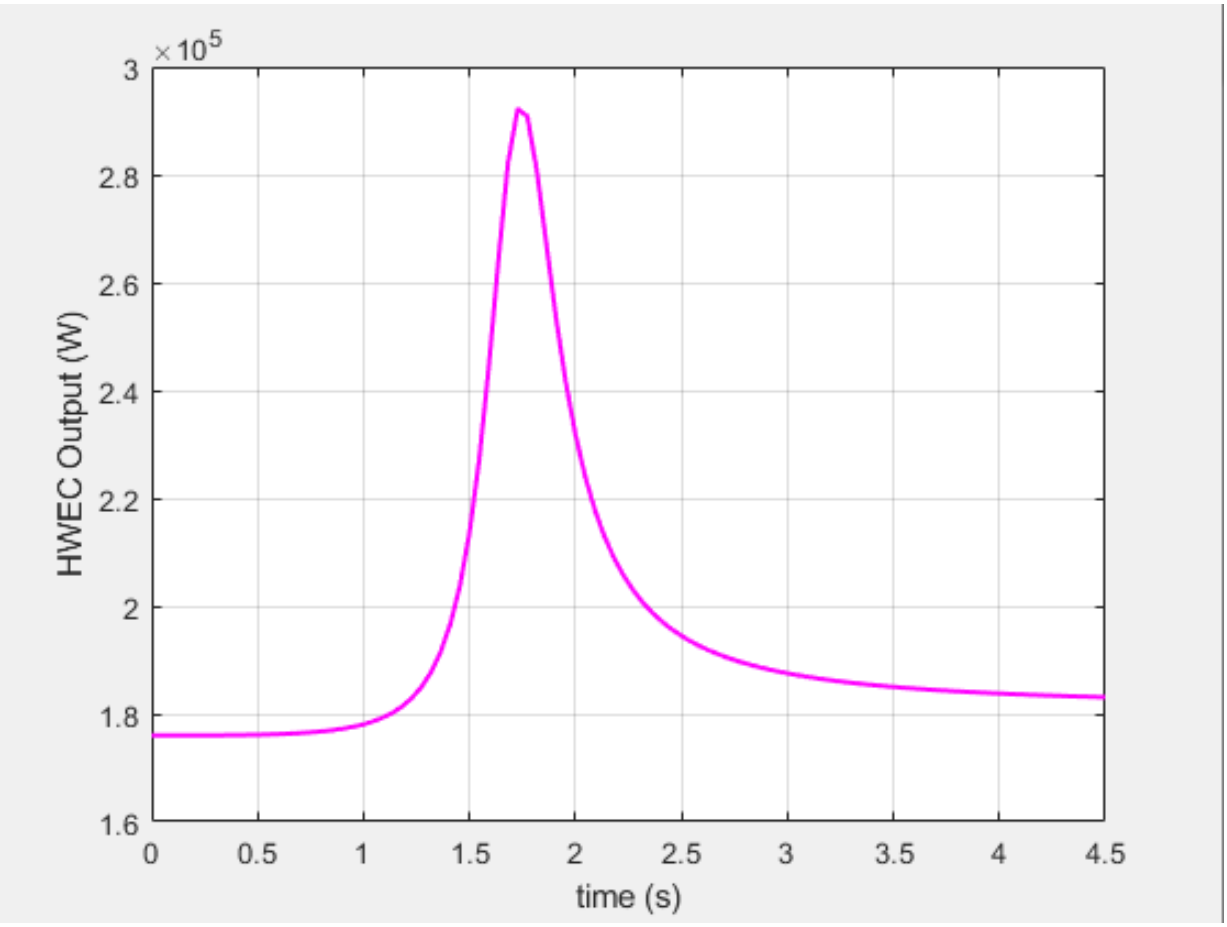


Fig. 11 Total Power Output Profile of the HWEC

The validation of the HWEC system developed for the Escravos region was conducted by comparing its performance indicators with data from existing literature on isolated WECs, solar power plants, and hybrid renewable energy systems. As shown in Table 3, the capacity factor results for the HWEC are presented and compared with other sources and wave tank experiments.

Table 3 indicates the Capacity factor and Absolute Mean Error of Various Hybrid Power Plants

Reference	Device type & Site	Capacity Factor	Absolute Mean Error
This research	Solar and WEC	40.4%	----
Ronkko *et al* (2023)	Wind and WEC	39%	1.4%
Arduino *et al* (2025)	Offshore wind Turbine and WEC	35.89%	4.51%
Das *et al* (2019)	Solar and Wind Turbine	42.1%	1.7%
Polo (2025)	Solar and Wind Turbine	38%	2.4%
NoviOcean HEC (2025)	WEC, Wind and Solar	40%	0.4%

Fig. 12 shows the power output against time of the WEC using WEC-SIM. The WEC-Sim results show close agreement with the PHK-ROS power output. The power output from the WEC-Sim was observed to be 2618W, while the PHK-ROS power output is 2641W, as shown in Fig. 6. These results show proximity, which agrees that the research model performance validity is reliable when compared to the WEC-Sim power output, as shown in Fig. 12.

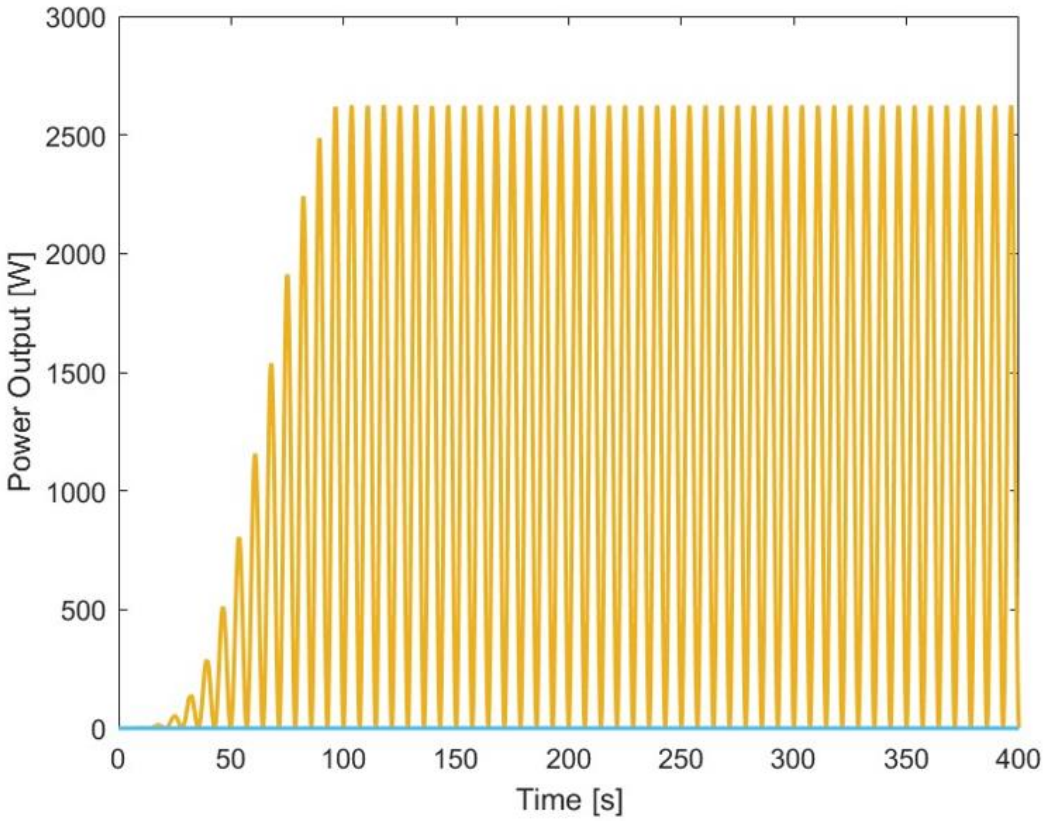


Fig. 12 WEC-Sim Power Output of the WEC

3.2 Discussion

To maximise the use of renewable energy from two different sources, the HWEC system integrates wave energy conversion and solar power generation. This combination uses the constant power production of the solar plant in combination with the cyclic nature of the wave energy. The main meta-ocean data used in this analysis are water depth of 1100 meters, wind speed of 15 to 20 m/s, wave height of 3.0 to 3.5 meters, and wave period of 15 to 17 seconds. These sources help in improving the overall power efficiency and reliability by cooperating with each other. High wave activity and high solar insolation are the natural conditions for the HWEC system, which is a sustainable way to address the needs of the energy sector. This analysis was done by using equations 1 to 13.

The device makes its best energy conversion at the wave crest (at about 1.1 to 3s). The WEC harvests the wave energy maximally, and this causes a peak in power generation. Using the PAIK-ROSS model, during the implementation of equations 1- 13, the power output of the WEC was analyzed. Above this peak, the power output falls from 3 to 4.5 seconds, and starts generating again as the wave heads for its trough, as shown in Fig. 4. The nonlinearity of the energy extraction is reflected in the results with fluctuating power output and slight changes in frequency in the optimum range. The process of calculating the average power of WEC is 2641W for one unit. A total of 116.204 kW of power will be generated from the forty-four WEC floaters that are shown on the structure.

The solar power plant results shown in Figs. 5 to 9 produced detailed plots of solar output fluctuations across critical months, with results ranging from 1.3 to 6.2 peak sun hours. Dry season months, particularly November to February, consistently have higher sunlight hours, with November having between 5.3 to 6.2 hours per day over the years. In contrast, June, July, and August - summer months - record the least sunlight hours. For instance, in July 2017, 1.4 hours of sunshine per day were received, leading to a substantial drop in energy output, making it hard to meet energy demands without additional storage or alternative power sources.

Yearly variations are also apparent. January is a good example of this, where sunlight hours amount to 4.0 hours per day in 2016, which significantly affects energy output. Initially, in April 2015, 5.9 hours of sunlight per day were recorded, and this fell to 3.8 hours in 2020, which led to a noticeable fall in energy production potential. Seasonal energy generation is characterized by the

fact that months with high solar hours, such as November, are suitable for energy-intensive applications. Months with lower hours of sunlight, such as July and August, may need backup solutions to make up for the lower energy generation.

This data puts into perspective the importance of taking into consideration seasonal and annual variations of sunlight when planning solar energy systems in order to have a reliable and constant energy supply. The results show efficient energy conversion and a stable power supply, as the values are almost constant in the graphs. This output is compared well with the solar panel output to be expected under stable operating conditions. The total power output of the HWEC is 292.2kW, as shown in Fig. 10. This shows that the hybrid system effectively combines the WEC and solar power plant.

The choice of 44 WECs and 440 solar panels is based on the available space on the platform and the ability to balance the PHK-ROS model WEC performance. A total weight of 53332.98 tonnes with a length of 71.99m and a breadth of 14.4m can only comfortably contain 440 solar panels on the platform surface, with each panel having a dimension of 1.956m in length and 1.21m in width. The 44 WEC yields 116kW (39% of the total power generated) peak power while the PV module provides 176kW (61% of the generated power) peak power during peak sunlight.

The result validation of Table 3 focuses on statistical indicators such as capacity factor, correlation coefficient, and absolute mean error. This result shows that there is a strong correlation when this research result is compared to other related work. The performance comparison with other studies in different environments helps to establish the novelty of the developed HWEC using the PAIK-ROS model. The power output of the WEC floater was validated using WEC-Sim as shown in Fig. 12. The total power using the PAIK-ROS model shows a close relationship with the total power output obtained using WEC-SIM.

4.0 Conclusion

This study shows the feasibility of a hybrid system with the combination of WEC and solar energy using PHK-ROS model for the WEC. A clear time-dependent behaviour is observed for the power output of the WEC, which decreases from 0 to 1 second and reaches a maximum between 1.1 and 3 seconds because of the optimal resonance with the wave motion. Energy is harvested as the wave passes through its trough, and power then decreases from 3 to 4.5 seconds. This trend is reflected in the average power of one WEC (2641 W). Solar energy analysis from more than six years of

data showed obvious seasonal variation, with November having the highest mean sun hours (5.4-6.2 hours/day) and July the lowest (1.4 hours/day). The system uses four hundred forty panels (each one with 500 W) and provides 176 kW and an average daily energy production of 928.46 kWh. The hybrid system has a constant power of 10.746 kW and a maximum power of 292.2 kW. WEC fluctuations improve the overall energy yield and help ensure an efficient and balanced renewable energy supply. The combination of the solar and WEC power plant enhances system-level performance by improving the capacity factor of the HWEC and ensuring greater availability of power compared to relying on a single renewable source.

References

Abam, T J; Agbakwuru, J A and Adeyemi, O I (2017) Numerical modeling of current on wave drift load of a ship shaped offshore structures (case study-Excraros in West African Offshore). *Journal of Mechanical and Civil Engineering. ISSN: 2456-1479 volume 3. pp. 22-40.*

Aderinto, T., and Li, H. (2018). Ocean Wave Energy Converters: Status and Challenges. *Energies*, *11*(5), 1250. https://doi.org/10.3390/en11051250

Ahamed, R., McKee, K., & Howard, I. (2022). A Review of the Linear Generator Type of Wave Energy Converters' Power Take-Off Systems. *Sustainability*, *14*(16), 9936. https://doi.org/10.3390/su1416993

Al-Rawashdeh, H., Al-Khashman, O. A., Al Bdour, J. T., Gomaa, M. R., Rezk, H., Marashli, A., Arrfou, L. M., and Louzazni, M. (2023). Performance Analysis of a Hybrid Renewable-Energy System for Green Buildings to Improve Efficiency and Reduce GHG Emissions with Multiple Scenarios. *Sustainability*, *15*(9), 7529. https://doi.org/10.3390/su15097529

Ambuhl, S., Kramer, M., and Sørensen, J. D. (2014). Reliability-Based Structural Optimization of Wave Energy Converters. *Energies*, *7*(12), 8178-8200. https://doi.org/10.3390/en7128178

Arduino, M. V., De Almeida, E., Loinaz, M., and Weschenfelder F. (2025). Hybrid Offshore Wind and Wave Energy Systems: A Case Study of Uruguay. Paper presented at the Offshore Technology Conference, Houston, Texas, USA. doi:

Bhattacharyya, S. (2021). "Stochastic modeling of wave-structure interactions." *Applied Ocean Research*, 106, 102422.

Cao, Y., Townsend, N., and Tan, M. (2017). Hybrid renewable energy system for ocean-going platforms. *OCEANS 2017 Aberdeen*.

Chen, P., and Wu, D. (2024). A review of hybrid wave-tidal energy conversion technology. *Ocean Engineering*.

Choi, Y., Rayl, J., Tammineedi, C., and Brownson, J.R.S. (2011) PV Analyst: Coupling ArcGIS with TRNSYS to assess distributed photovoltaic potential in urban areas. *Sol. Energy*, 85, 2924–2939.

Cui, L., Amani, S., Gabr, M., Kumari, W. G. P., Ahmed, A., Ozcan, H., Horri, B. A., and Bhattacharya, S. (2024). Synergistic Hybrid Marine Renewable Energy Harvest System. *Energies*, *17*(5), 1240. https://doi.org/10.3390/en17051240

Das K., Anca D, Vangari D, Koivisto M, Sorensen P & Altin M. (2019). Enhanced Features of Wind-Based Hybrid Power Plants. Conference: 4th International Hybrid Power Systems Workshop, Crete, Greece.

Del R, B., Choupin, O., Melián-Martel, N., & Schallenberg-Rodriguez, J. (2024). Application of a revised integration of methods for wave energy converter and farm location pair mapping. *Energy Conversion and Management*.

Dumkhana, L and Idoniboyeobu, D.C. (2018). Solar PV/Battery System Analysis for Faculty of Engineering Building, Rivers State University, Port Harcourt, Nigeria. *IOSR Journal of Electrical and Electronics Engineering (IOSR-JEEE)*, 45-51.

Falnes, J. (2002). *Ocean Waves and Oscillating Systems*. Cambridge University Press.

Felix, A., V. Hernández-Fontes, J., Lithgow, D., Mendoza, E., Posada, G., Ring, M., & Silva, R. (2019). Wave Energy in Tropical Regions: Deployment Challenges, Environmental and Social Perspectives. *Journal of Marine Science and Engineering*, *7*(7), 219. https://doi.org/10.3390/jmse7070219

Franklin E. (2017). Solar Photovoltaic Site Assessment. Retrieved from Cooperative Extension: http://extension.arizona.edu/site/extension.Arizona.edu/files/pubs/az1697-2017.pdf

Guo, B., Zheng, S., Ringwood, J., Henriques, J., & Zhang, D. (2021). Guest Editorial: Advances in Wave Energy Conversion Systems. *IET Renewable Power Generation*.

https://interestingengineering.com/energy/hybrid-energy-raft-power-1000-homes-daily. Retrievd on the 23rd of October, 2025.

https://sinay.ai/en/what-is-floating-wind/.Retrievd on the 12th of December, 2025.

Jierula A., Wang S. H., and Wang P. (2021). Study on Accuracy Metrics for Evaluating the Predictions of Damage Locations in Deep Piles Using Artificial Neural Networks with Acoustic Emission Data. *Applied Sciences*, 11(5), 2314-2321.

Khatib, T., and Muhsen, D. H. (2020). Optimal Sizing of Standalone Photovoltaic System Using Improved Performance Model and Optimization Algorithm. *Sustainability*, *12*(6), 2233. https://doi.org/10.3390/su12062233

Khurshid, H., Mohammed, B. S., Al-Yacouby, A. M., Liew, M. S., and Zawawi, N. A. W. A. (2024). Analysis of hybrid offshore renewable energy sources for power generation: A literature review of hybrid solar, wind, and waves energy systems. *Developments in the Built Environment*.

Korda, M., and Mezić, I. (2018). "Linear predictors for nonlinear dynamical systems: Koopman operator theory." *Applied Energy*, 211, 112–125.

Koutrouveli, T. I., Di Lauro, E., das Neves, L., Calheiros-Cabral, T., Rosa-Santos, P., and Taveira-Pinto, F. (2021). Proof of Concept of a Breakwater-Integrated Hybrid Wave Energy Converter Using a Composite Modelling Approach. *Journal of Marine Science and Engineering, 9*(2), 226.

Majeed Y, Muhammad U K, Muhammad W, Umair Z, Faisal M, Faizan M, Muhammad S and Ali R. (2023). Renewable energy as an alternative source for energy management in agriculture, *Energy Reports*, 10(1), 344-359, ISSN 2352-4847.

Ndiaye, A., Moussa, M. S., Dione, C., Sawadogo, W., Bliefernicht, J., Dungall, L., and Kunstmann, H. (2022). Projected Changes in Solar PV and Wind Energy Potential over West Africa: An Analysis of CORDEX-CORE Simulations. *Energies*, *15*(24), 9602. https://doi.org/10.3390/en15249602

Nwaorgu G.O and Ogbonnaya E. A. (2023). Evaluation of an Alternative Source of Power for Ship Operations in Ports. *Journal of Engineering, Emerging Technologies and Applied Sciences (JEETAS).* 1(1), 2-12.

O'Dwyer, J., and Ringwood, J. V. (2020). "Port-Hamiltonian modeling of wave energy converters." *IEEE Transactions on Sustainable Energy*, 11(3), 1452–1460.

Ogbeibu, A. and Oribhabor, B. (2023). The Niger Delta Mangrove Ecosystem and Its Conservation Challenges. *Intech Open* 1-23, 10.5772/intechopen.112543.

Phillips, R. E. (2019). Harvesting Ocean Wave Energy: A Proposed System for Conversion into Electrical Power. *Natural Gas and Electricity*.

Podder, S., Khan, R.S. and Mohon, S. Md A.A. (2015). The Technical and Economic Study of Solar-Wind Hybrid Energy System in Coastal Area of Chittagong, Bangladesh. *Journal of Renewable Energy*. 1-10. http://dx.doi.org/10.1155/2015/482543

Polo, J. (2025). Hybrid Wind–Solar Generation and Analysis for the Iberian Peninsula: A Case Study. *Energies*, *18*(15), 3966. https://doi.org/10.3390/en18153966

Ronkko, J., Khosravi, A., and Syri, S. (2023). Techno-Economic Assessment of a Hybrid Offshore Wind–Wave Farm: Case Study in Norway. *Energies*, *16*(11), 4316. https://doi.org/10.3390/en16114316

Sabzehgar, R., and Moallem, M. (2009). A review of ocean wave energy conversion systems. *2009 IEEE Electrical Power and Energy Conference (EPEC)*.

Silverio, N. M., Barros, R. M., Tiago F. G., Redon-Santafe, M., Dos-Santos, I. F.S., and De-Mello V. E. (2018). Use of Floating PV Plants for Coordinated Operation with Hydropower Plants, Case Study of the Hydroelectric Plants of the Sao Francisco Rivers Basin. *Energy Conversion Management.* 171, 339-349.

Strielkowski, W., Civín, L., Tarkhanova, E., Tvaronavičienė, M., and Petrenko, Y. (2021). Renewable Energy in the Sustainable Development of the Electrical Power Sector: A Review. *Energies*, *14*(24), 8240. https://doi.org/10.3390/en1424824